Experiments on Chaotic Vibrations of a Stepped Beam

Shinichi MARUYAMA, Ken-ichi NAGAI and Tatsuya INOUE
Department of Mechanical System Engineering, Graduate School of Engineering, Gunma University, 1-5-1 Tenjin-cho, Kiryu, Gunma 376-8515, JAPAN, maruyama@gunma-u.ac.jp

1. Introduction Experimental results are presented on chaotic vibrations of a stepped beam constrained by an axial elastic spring. The rectangular cross section of the beam changes to H shaped at the mid span of the beam. One end of the beam is clamped and the other is simply-supported. The beam is compressed to the post-buckled state by the spring in the axial direction. The post-buckled beam is excited laterally under periodic acceleration. The dynamic responses of the beam are measured under the effect of axial compression. In typical frequency ranges, chaotic responses are observed. The responses are inspected with the Fourier spectra, the Poincaré maps, the maximum Lyapunov exponents and the Karhunen-Loève transformation.

2. Test beam and Test Procedure Fig.1 shows the stepped beam and its fixture at both ends. A thin phosphor bronze beam with thickness h=0.30 mm, breadth b=40 mm and length L=140 mm is clamped at one end and simply-supported at the other end. Four thin phosphor bronze beam (thickness 0.31 mm, breadth 4.9 mm, length 34 mm) are attached to the mid span of the beam, then the cross section is locally changed to H-shaped. At the simply-supported end, the beam is connected to an elastic plate by the strips of adhesive films. The elastic plate is clamped by the slide block and works as the axial spring. The beam is compressed by the axial spring, then the beam is deformed to the post-buckled configuration. To find fundamental properties of the beam, the linear natural frequencies and the restoring force are inspected. The post-buckled beam is excited laterally with an electromagnetic exciter. The beam is subjected to gravitational acceleration and periodic acceleration $a_d \cos 2\pi f\, t$, where f is the excitation frequency and a_d is the peak amplitude of acceleration. The dynamic responses of the beam are measured under three magnitudes of axial compression. In typical frequency ranges, chaotic responses are observed. The responses are inspected with the frequency response curves, the Fourier spectra, the Poincaré projections and the maximum Lyapunov exponents. The contribution of vibration mode to the chaos is discussed with the Karhunen-Loève transformation.

3. Results and Discussion The experimental results are arranged with the following non-dimensional notations.

$$\xi = x/L,\quad w = W/h,\quad [p_s, p_d] = [g, a_d]\rho AL^4/EIr,\quad q_s = Q_s L^3/EIr,\quad n_x = N_x L^2/EI,$$
$$n_c = n_x/n_{cr},\quad \omega = 2\pi f/\Omega_0,\quad \tau = \Omega_0 t,\quad r = \sqrt{I/A},\quad \Omega_0 = L^{-2}\sqrt{EI/\rho A} \qquad (1)$$

where r represents the radius of gyration of cross section of the beam, Ω_0 is the coefficient corresponding to lateral vibration of the beam. In Eq. (1), ξ is the non-dimensional coordinate, w is the lateral displacement normalized by the beam thickness h. Notation n_x is the non-dimensional axial force where N_x represents the axial force on the cross section. The symbol n_c is the non-dimensional axial force, normalized by the non-dimensional buckling resultant n_{cr} = -18.4. Notations p_s and p_d are the non-dimensional load intensities related to the accelerations of gravity g and of the periodic peak amplitude a_d , respectively, which are chosen as p_s=0.42×10^3 and p_d= 0.86×10^3. When the characteristics of restoring force of the beam is examined, static lateral deflection by the concentrated static force Q_s is measured. Notation q_s is the non-dimensional static force. Notations ω and τ are the non-dimensional exciting frequency and the time, respectively.

Figure 2 shows the linear natural frequencies ω_1, ω_2 of the beam under the axial compressive force $-n_x$ by the spring. Increasing the compressive force from n_x = 0, the lowest linear natural frequency decreases gradually. Increasing the axial force from $-n_{cr}$= 18.4, the lowest natural frequency increases steeply because of the post-buckled deformation of the beam, which has an

initial deflection. Fig. 3 shows the static lateral deflection w of the beam under the concentrated force q_s loaded on the center of the beam. The characteristics of restoring force of the beam show the type of a softening-and-hardening spring including negative gradient. At the axial compression n_c =1.17, the beam has two static equilibrium points. The range of deflection, where the negative gradient appears, decreases as the axial compression is decreased.

Figure 4 shows the nonlinear response curves of the post-buckled beam. The amplitude of response at the position ξ= 0.65 is shown with the root-mean-square value. The resonance response is denoted by the symbol (i: j) with the mode of vibration i and the type of resonance j. For example, j = 1 and j = 1/2 represent the principal resonance and the sub-harmonic resonance of 1/2 order, respectively. The chaotic response is represented by the symbol C. Natural frequencies of the post-buckled beam are also indicated by the solid circles on the abscissa. In the figure, the nonlinear response curve corresponds to the characteristics of restoring force with the type of a softening-and-hardening spring. Under the axial compression n_c = 1.17 and 1.15, the chaotic responses are generated from the non-resonant response with the jump phenomenon, as the excitation frequency is decreased. In contrast, under the axial compression n_c = 1.10, the sub-harmonic resonance of 1/2 order continuously transit to the chaotic responses by decreasing the excitation frequency. Fig. 5 shows the chaotic response C1 of the post-buckled beam, under the excitation frequency ω_{ex} =12.0, and the axial compression n_c = 1.17. In Fig. 5(a), the time progress of the response w is presented by the number of excitation period τ_e . The chaotic response is dominated by dynamic snap-through. The Fourier spectrum in Fig. 5(b) shows broad-band spectrum. Dominant peaks of the spectrum correspond to the ultra-sub harmonic resonance of 2/3 order with the lowest mode of vibration. In Fig. 5(c), the Poincaré projection is shown in the space of deflection and velocity. A fractal pattern is clearly constructed in this Poincaré projection. Fig. 6 shows the chaotic response C under ω_{ex} =11.7 and n_c = 1.15. Among the broad-band spectrum in Fig. 6(b), dominant peaks of the spectrum correspond to the sub-harmonic resonance of 1/2 order and the ultra-sub harmonic resonance of 3/4 order with the lowest mode of vibration. Figure 7 shows the chaotic response C under ω_{ex} =16.2 and n_c = 1.10. The Fourier spectrum shows fewer dominant peaks in Fig. 7(b). The most dominant peak of the spectrum corresponds to the sub-harmonic resonance of 1/2 order with the lowest mode of vibration. In Fig. 7(c), the point of the Poincaré projection is widely distributed in two parts. In each part, clear fractal pattern can be observed. Fig. 8 show the maximum Lyapunov exponents λ_{max} related to the embedding dimension e of the chaotic responses. Since the maximum Lyapunov exponents converge to positive values, these responses are confirmed as chaos. As the axial compression n_c is increased from n_c = 1.10 to n_c = 1.17, the maximum Lyapunov exponent increases from λ_{max} = 0.5 to λ_{max} = 1.5. The Karhunen-Loève transformation enables one to estimate the contribution of vibration modes to the chaotic response. The results are summarized in Table 1. Modal patterns and corresponding contribution ratio are shown in the table. The lowest mode of vibration has the largest contribution to the chaotic responses more than 99.8 %. As the axial compression is increased, the contribution of the second mode of vibration increases.

4. Conclusion Experimental results are presented on chaotic vibrations of a stepped beam. As the axial compression to the beam is increased, the maximum Lyapunov exponents converge to larger value, and contribution of the second vibration modes to the chaotic response increases.

References

1) Ken-ichi NAGAI, Shinichi MARUYAMA, Kazuya SAKAIMOTO and Takao YAMAGUCHI. Experiments on Chaotic Vibrations of a Post-buckled Beam with an Axial Elastic Constraint, *Journal of Sound and Vibration*, Vol.304 (2007) pp. 541-555.

2) Dai YANAGISAWA, Ken-ichi NAGAI and Shinichi MARUYAMA. Chaotic Vibrations of a Clamped Supported Beam with a Concentrated Mass Subjected to Static Axial Compression and Periodic Lateral Acceleration, *Journal of System Design and Dynamics*, Vol. 2,No. 3, (2008) pp. 762-773.

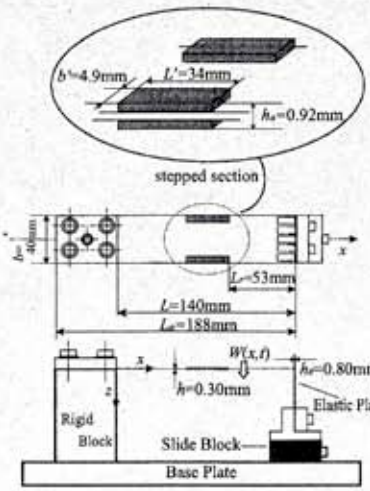

Fig. 1 Stepped beam and fixture

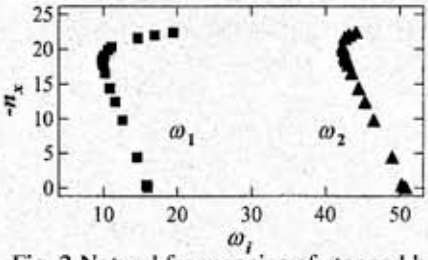

Fig. 2 Natural frequencies of stepped beam

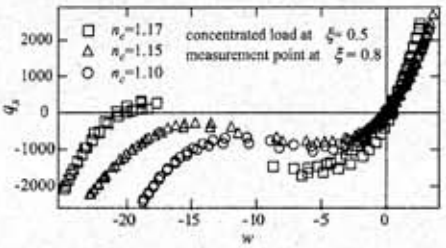

Fig. 3 Characteristics of restoring force

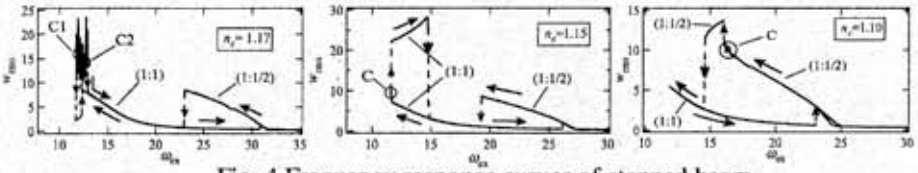

Fig. 4 Frequency response curves of stepped beam

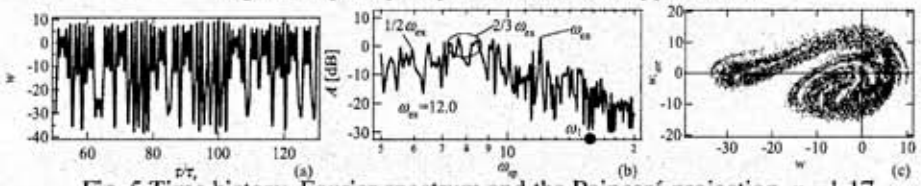

Fig. 5 Time history, Fourier spectrum and the Poincaré projection, n_c=1.17

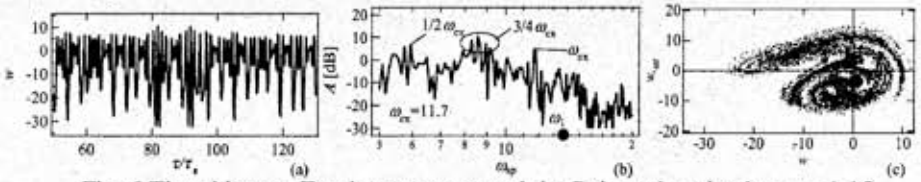

Fig. 6 Time history, Fourier spectrum and the Poincaré projection, n_c=1.15

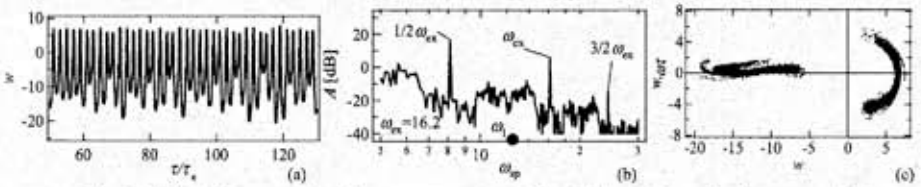

Fig. 7 Time history, Fourier spectrum and the Poincaré projection, n_c=1.10

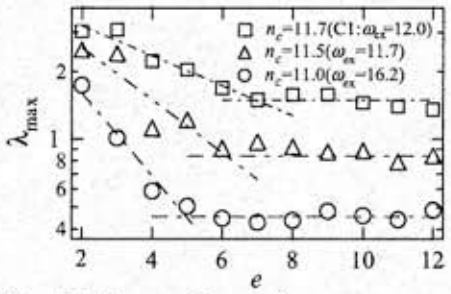

Fig. 8 The maximum Lyapunov exponent related to embedding dimension

Table 1 Results of the Karhunen-Loève transformation

Order of eigenvalues i	1	2	3	4
	Contribution ratio (%)			
n_c=11.7 C1	99.8	0.149	1.85×10^{-2}	6.41×10^{-4}
n_c=11.5	99.9	0.104	2.06×10^{-2}	6.47×10^{-4}
n_c=11.0	99.9	8.20×10^{-2}	1.78×10^{-2}	9.42×10^{-4}